JOURNAL OF AIRCRAFT
Vol. 33, No. 2, March–April 1996

# Semianalytical Sensitivity of Floquet Characteristic Exponents with Application to Rotary-Wing Aeroelasticity

Ih-Cheng Shih,* Anne Marie Spence,* and Roberto Celi†
*University of Maryland, College Park, Maryland 20742-3015*

**The stability of a nonlinear dynamic system with periodic coefficients can be evaluated by linearizing the equations of motion of the system about a steady-state equilibrium position and then, using Floquet–Liapunov theory, by calculating the eigenvalues, or characteristic multipliers, of the transition matrix at the end of one period, and finally by examining the real parts of the characteristic exponents corresponding to the characteristic multipliers. This article describes a methodology to calculate the sensitivity of the characteristic exponents to changes in system parameters, taken as design variables, using semianalytic derivatives rather than finite difference approximations. Linear and nonlinear contributions to such sensitivities are identified and algorithms for the calculation of each contribution are provided. The linear contribution to the sensitivity to each design variable can be calculated at a fraction of the cost of one analysis, with appropriate attention to the details of the computer implementation. The nonlinear contribution requires a fixed overhead cost of as many analyses as the number of variables that define the equilibrium position, regardless of the number of design variables with respect to which the sensitivities are sought. A potential problem in the calculation of finite difference gradients is identified and discussed. The linear portion alone is sufficiently accurate for the helicopter problem of the study.**

## Nomenclature

$[B(\psi)]$ = linearized state matrix of the periodic system
$GJ$ = torsion stiffness of the blade
$N_{DV}$ = number of design variables
$n$ = number of states
$n_T$ = number of parameters defining the equilibrium position of the system
$p$ = generic design variable
$\boldsymbol{q}$ = vector defining the trim state of the helicopter
$T$ = common period of the coefficients of the system
$\boldsymbol{v}_i, \boldsymbol{w}_i$ = $i$th left and right eigenvector of the Floquet transition matrix at the end of one period
$z$ = vector containing the transition matrix stored columnwise
$\zeta_i$ = real part of the $i$th characteristic exponent
$\Lambda_i$ = $i$th characteristic multiplier of the Floquet transition matrix at the end of one period
$\lambda_i$ = $i$th characteristic exponent of the Floquet transition matrix at the end of one period
$\mu$ = advance ratio, aircraft speed divided by rotor hover tip speed
$[\Phi(2\pi)]$ = Floquet transition matrix at the end of one period
$\psi$ = blade azimuth angle, used as nondimensional time
$\omega_i$ = imaginary part of the $i$th characteristic exponent

*Subscripts*
$I$ = imaginary part
$R$ = real part

*Superscript*
$*$ = derivative with respect to $\psi$

## Introduction

THE stability of a dynamic system described by linear ordinary differential equations (ODE) with periodic coefficients can be evaluated using Floquet–Lyapunov theory, by calculating the characteristic exponents of the Floquet transition matrix (FTM) of the system. Such systems arise, for example, from the formulation of aeroelastic stability problems for helicopters in forward flight. In this case the system of ODE is nonlinear and is linearized about an equilibrium (or trim) position. In the solution of optimization problems with aeroelastic stability constraints, the gradients of the characteristic exponents with respect to each of the design variables are typically required. Because the mathematical models necessary for accurate stability calculations tend to be very complex, such gradients are often calculated using finite difference approximations that are easy to implement, but are computationally inefficient. For this reason there has been a growing interest in analytical or semianalytical methods for gradient calculations.

Only two stability sensitivity analyses are available in the literature for a system with periodic coefficients. The first is from Lim and Chopra,[1] who derive analytical expressions for the gradients of the characteristic exponents with respect to several mass and structural design parameters of the rotor. The underlying stability analysis is for a fixed shaft condition. A finite element model is used, directly based on Hamilton's principle. In the second, from Lu and Murthy,[2] analytical sen-

Presented as Paper 94-1544 at the AIAA 35th Structures, Structural Dynamics, and Materials Conference, Hilton Head, SC, April 18–20, 1994; received June 26, 1994; revision received July 17, 1995; accepted for publication Sept. 22, 1995. 

*ARO Graduate Fellow, Center for Rotorcraft Education and Research and Institute for Systems Research, Department of Aerospace Engineering.

†Associate Professor, Center for Rotorcraft Education and Research and Institute for Systems Research, Department of Aerospace Engineering. Senior Member AIAA.

sitivities are also derived. The equivalent of a modal coordinate transformation, based on the complex eigenvectors of the homogeneous system, is then used as the basic idea for the method. Thanks to this transformation, the sensitivities with respect to each design parameters are calculated independently, instead of in a coupled way as in Ref. 1. The method is applied to two simple helicopter models, namely a coupled rotor–fuselage system in hover and an isolated rotor blade in forward flight. Both Refs. 1 and 2 neglect possible changes of the characteristic exponents because of changes in the equilibrium position about which the nonlinear equations of motion are linearized.

The main objective of this article is to present a semianalytic method for the calculation of the gradients of the characteristic exponents with respect to generic design variables. The method is called semianalytic because, although the starting point is an analytic chain-rule differentiation of the characteristic exponents, several intermediate quantities are calculated using finite difference approximations. The effects of changes in the equilibrium position about the equations are linearized and taken into account. The underlying analysis is a coupled rotor–fuselage aeromechanic stability analysis.

## Solution Method

The characteristic multipliers $\Lambda_i$ are the eigenvalues of the FTM $[\Phi(2\pi)]$ at the end of one period.[3] The characteristic exponents $\lambda_i$ are related to the characteristic multipliers by

$$\exp(\lambda_i T) = \Lambda_i \qquad i = 1, 2, \ldots, n \tag{1}$$

so that, if $\lambda_i = \zeta_i + i\omega_i$ and $\Lambda_i = \Lambda_{Ri} + i\Lambda_{Ii}$, one has

$$\zeta_i = (1/2T)\ell n(\Lambda_{Ri}^2 + \Lambda_{Ii}^2) \qquad \omega_i = (1/T)\tan^{-1}(\Lambda_{Ii}/\Lambda_{Ri}) \tag{2}$$

The system is stable if all of the real parts $\zeta_i$ of the characteristic exponents are negative. In this study the common period $T$ is equal to one rotor revolution and $T = 2\pi$. We are interested in the derivative of the characteristic exponent $\lambda_i$ with respect to $p$. For example,

$$\frac{d\lambda_i}{dp} = \frac{d\zeta_i}{dp} + i\frac{d\omega_i}{dp} \tag{3}$$

Using Eq. (2), the sensitivity of the characteristic exponents can be related to the sensitivity of the characteristic multipliers by

$$\frac{d\zeta_i}{dp} = \frac{1}{T}\left(\frac{\Lambda_{Ri}}{\Lambda_{Ri}^2 + \Lambda_{Ii}^2}\frac{d\Lambda_{Ri}}{dp} + \frac{\Lambda_{Ii}}{\Lambda_{Ri}^2 + \Lambda_{Ii}^2}\frac{d\Lambda_{Ii}}{dp}\right) \tag{4}$$

$$\frac{d\omega_i}{dp} = \frac{1}{T}\left(-\frac{\Lambda_{Ii}}{\Lambda_{Ri}^2 + \Lambda_{Ii}^2}\frac{d\Lambda_{Ri}}{dp} + \frac{\Lambda_{Ri}}{\Lambda_{Ri}^2 + \Lambda_{Ii}^2}\frac{d\Lambda_{Ii}}{dp}\right) \tag{5}$$

The FTM $[\Phi(2\pi)]$ is a real nonsymmetric matrix. Therefore, it can be shown[4] that the sensitivity of its $i$th eigenvalue, which is the $i$th characteristic multiplier, is

$$\frac{d\Lambda_i}{dp} = \frac{d\Lambda_{Ri}}{dp} + i\frac{d\Lambda_{Ii}}{dp} = \frac{v_i^T \dfrac{d[\Phi(2\pi)]}{dp} w_i}{v_i^T w_i} \tag{6}$$

where $v_i$ and $w_i$ are, respectively, the left and right eigenvectors of the FTM $[\Phi(2\pi)]$ corresponding to the eigenvalue $\Lambda_i$. In general, both $v_i$ and $w_i$ are complex-valued vectors. For a nonlinear system, the FTM is obtained by linearizing the equations of motion about an equilibrium position. In rotary-wing aeroelasticity problems, this equilibrium position corresponds to a trimmed state for the rotor and the fuselage. In general, a change in the design parameter $p$ will also affect the FTM indirectly, that is, through a change in the equilibrium position about which the equations are linearized. In the remainder of this article the direct effect of changes in $p$ will be referred to as the linear effect, whereas the indirect will be referred to as the nonlinear effect. Therefore, if $q$ is the vector definining the equilibrium position about which the nonlinear ODE are linearized, the sensitivity of the FTM with respect to $p$ will be given by

$$\frac{d[\Phi(2\pi)]}{dp} = \frac{\partial[\Phi(2\pi)]}{\partial p} + \sum_{k=1}^{nT}\frac{\partial[\Phi(2\pi)]}{\partial q_k}\frac{\partial q_k}{\partial p} \tag{7}$$

In typical helicopter problems, the various components $q_k$ of the vector $q$ describe the trim state of the aircraft and the steady-state motion of the blades. They include, for example, the trim values of pitch control settings, angular velocities and aerodynamic angles of attack of the aircraft, and also the harmonics of the motion of the blades in flap bending, lag bending, and torsion degrees of freedom. The first term in Eq. (7) is the change in FTM because of a change in $p$ calculated for the same equilibrium position as the baseline design. The summation in Eq. (7) represents the changes of the FTM due to the changes in the equilibrium position, about which the equations are linearized, caused by changes in $p$. The terms in the summation are calculated for the baseline design and are all equal to zero for linear dynamic systems.

### Linear Contribution

As a preliminary to the calculation of the various sensitivities of the FTM in Eq. (7), recall that the FTM at the end of one period $[\Phi(2\pi)]$ can be calculated as follows.[5] Let $z_k(2\pi)$ be the $k$th column of the FTM, and define a vector $z$ as

$$z(\psi) = \begin{Bmatrix} z_1(\psi) \\ z_2(\psi) \\ \vdots \\ z_n(\psi) \end{Bmatrix} \tag{8}$$

Then solve the system

$$\overset{*}{z} = [D(\psi)]z \tag{9}$$

from $\psi = 0$ to $\psi = 2\pi$, with initial conditions

$$z(0) = \begin{Bmatrix} e_1(\psi) \\ e_2(\psi) \\ \vdots \\ e_n(\psi) \end{Bmatrix} \tag{10}$$

where $e_k$ is a vector of size $n$ with all of its elements equal to zero except for the $k$th, which is equal to one. The matrix $[D(\psi)]$ is an $n^2$ by $n^2$ block–diagonal matrix, in which all of the $n$ blocks are identical, i.e.,

$$[D(\psi)] = \text{diag}[[B(\psi)][B(\psi)] \cdots [B(\psi)]] \tag{11}$$

The matrix $[B(\psi)]$ is the state matrix of the linearized system. The solution vector $z(2\pi)$ of Eq. (9) is the FTM $[\Phi(2\pi)]$ at the end of one period arranged columnwise, therefore the sensitivities of $[\Phi(2\pi)]$ are known if the sensitivities of $z(2\pi)$ are known.

The first sensitivity that appears in Eq. (7) is $\partial[\Phi(2\pi)]/\partial p$, which is a matrix that, when arranged columnwise, is identical to $\partial z(2\pi)/\partial p$. To obtain the latter derivative, rewrite Eq. (9) as

$$\overset{*}{z} - [D(\psi)]z = 0 \tag{12}$$

take derivatives with respect to $p$ and rearrange them to obtain

$$\frac{\partial^2 z}{\partial p \partial \psi} - [D(\psi)]\frac{\partial z}{\partial p} = \frac{\partial [D(\psi)]}{\partial p} z \tag{13}$$

define now

$$z_1 = \frac{\partial z(\psi)}{\partial p} \tag{14}$$

and rewrite Eq. (13) as

$$\overset{*}{z}_1(\psi) - [D(\psi)]z_1(\psi) = \frac{\partial [D(\psi)]}{\partial p} z \tag{15}$$

The initial condition for the vector $z_1$ is $z_1(0) = 0$. In fact, the process of calculating the FTM requires that $z(0)$ always be as indicated in Eq. (10), regardless of the value of $p$. This implies that the derivative of $z$ with respect to $p$, namely $z_1$, must be zero at $\psi = 0$. Equations (9) and (15) can be written together in matrix form as

$$\begin{Bmatrix} \overset{*}{z} \\ \overset{*}{z}_1 \end{Bmatrix} = \begin{bmatrix} D(\psi) & 0 \\ \dfrac{\partial D(\psi)}{\partial p} & D(\psi) \end{bmatrix} \begin{Bmatrix} z \\ z_1 \end{Bmatrix} \tag{16}$$

The integration of Eq. (16) from $\psi = 0$ to $\psi = 2\pi$ will yield simultaneously the FTM at the end of one period and its derivative with respect to $p$ for fixed equilibrium position. By the same argument one can show that to obtain the sensitivities with respect to $N_{DV}$ design variables $p_i$, $i = 1, \ldots, N_{DV}$, the following system of ODE needs to be solved:

$$\begin{Bmatrix} \overset{*}{z} \\ \overset{*}{z}_1 \\ \overset{*}{z}_2 \\ \vdots \\ \overset{*}{z}_{N_{DV}} \end{Bmatrix} = \begin{bmatrix} D(\psi) & 0 & 0 & \cdots & 0 \\ D(\psi) & \dfrac{\partial D(\psi)}{\partial p_1} & 0 & \cdots & 0 \\ D(\psi) & 0 & \dfrac{\partial D(\psi)}{\partial p_2} & \cdots & 0 \\ \vdots & \vdots & \vdots & & \vdots \\ D(\psi) & 0 & 0 & \cdots & \dfrac{\partial D(\psi)}{\partial p_{N_{DV}}} \end{bmatrix} \begin{Bmatrix} z \\ z_1 \\ z_2 \\ \vdots \\ z_{N_{DV}} \end{Bmatrix} \tag{17}$$

The various vectors $z_i(2\pi)$, $i = 1, \ldots, N_{DV}$ are the partial derivative matrices of the FTM with respect to the $i$th design variable, arranged columnwise. It may be interesting to notice that Eq. (17) is identical to the result obtained in Ref. 1, although several aspects of the derivation are different.

The mathematical format used for Eqs. (16) and (17) may give the misleading impression that the order of the system of ODE to be solved is equal to the number of states multiplied by $N_{DV} + 1$, and therefore, that the computational cost increases dramatically with the number of design variables (Ref. 2). That this is basically not true becomes clear when one considers an actual implementation composed of the following steps:

1) Solve Eq. (9); at each time (or $\psi$) step, calculate the sensitivity matrices $\partial D(\psi)/\partial p_i$ together with the state matrix $D(\psi)$, and accumulate them as required to build Fourier series expansions of both types of matrices over one period. Also prepare a Fourier series expansion of the solution $z(\psi)$.

2) Solve as many matrix equations like Eq. (15) as there are design variables, with a zero vector of initial conditions. All of the vectors and matrices required for the solution are reconstructed from the Fourier series expansions generated in the previous step. These matrix equations are decoupled and can be solved independently. The order of each of them is the same as the order of the original system.

The main reason for the misleading impression is that Eqs. (16) and (17) seem to indicate that the calculation of the baseline solution $z(\psi)$ is coupled with the calculation of the perturbed solutions $z_i(\psi)$. In reality $z(\psi)$ is completely decoupled from the sensitivity calculations and it can be considered as already known when the sensitivity calculations are performed. In fact, with a little care in the synchronization of the ODE solution, Eq. (17) can even be implemented in a form consistent with the following mathematical format:

$$\begin{Bmatrix} \overset{*}{z} \\ \overset{*}{z}_1 \\ \overset{*}{z}_2 \\ \vdots \\ \overset{*}{z}_{N_{DV}} \end{Bmatrix} = \begin{bmatrix} [D(\psi)] & 0 & 0 & \cdots & 0 \\ 0 & \dfrac{\partial D(\psi)}{\partial p_1} & 0 & \cdots & 0 \\ 0 & 0 & \dfrac{\partial D(\psi)}{\partial p_2} & \cdots & 0 \\ \vdots & \vdots & \vdots & & \vdots \\ 0 & 0 & 0 & \cdots & \dfrac{\partial D(\psi)}{\partial p_{N_{DV}}} \end{bmatrix} \times \begin{Bmatrix} z \\ z_1 \\ z_2 \\ \vdots \\ z_{N_{DV}} \end{Bmatrix} + \begin{Bmatrix} 0 \\ D(\psi)z \\ D(\psi)z \\ \vdots \\ D(\psi)z \end{Bmatrix} \tag{18}$$

in which the vector $D(\psi)z$ is obtained from the solution of the first row of the matrix equation and is treated as a known quantity in the solution of the subsequent rows.

It is clear that the key ingredient for the computational efficiency of the method is the ability to calculate the sensitivity matrices $\partial D(\psi)/\partial p_i$ for a cost that is less than the cost of calculating $[D(\psi)]$. In the present study, the cost of calculating a sensitivity matrix is about 5–10% of the cost of calculating $[D(\psi)]$. This is accomplished using special properties of the method of formulating the equations of motion, as shown in Ref. 6.

### Nonlinear Contribution

Consider now the terms in the summation of Eq. (7), which are associated with the nonlinearity of the problem. The terms $\partial q_k/\partial p$, $k = 1, \ldots, n_T$ describe the first-order change in equilibrium position of the system because of a change in $p$. They are calculated for the baseline configuration. In rotary-wing aeroelasticity, these terms collectively represent the change in trim state because of changes in $p$ and can be calculated very efficiently.[6] The derivative matrices $\partial[\Phi(2\pi)]/\partial q_k$, $k = 1, \ldots, n_T$ represent the change in the FTM at the end of one period due to a change in the equilibrium position about which the linearization of the governing ODE is carried out. To evaluate these matrices the time-varying matrices $\partial B(\psi)/\partial q_k$, $k = 1, 2, \ldots, n_T$ are required. These time-dependent matrices represent the sensitivities of the linearized system matrix with respect to changes in the equilibrium position about which the linearization is carried out. Note that the matrices are not dependent on $p_i$. Therefore, they can be calculated once and reused for all the design parameters of the problem. From a computational standpoint it is convenient to calculate them numerically at a sufficient number of azimuth angles using the finite difference approximations, build Fourier series expansions, and use the expansions in all the subsequent calculations. For example,

$$\frac{\partial B(\psi)}{\partial q_k} = B_0^k + \sum_{n=1}^{nD} (B_{nc}^k \cos n\psi + B_{ns}^k \sin n\psi) \tag{19}$$

where

$$\begin{Bmatrix} B_0^k \\ B_{nc}^k \\ B_{ns}^k \end{Bmatrix} = \frac{1}{2\pi}\int_0^{2\pi} \frac{\partial B(\psi)}{\partial q_k} \begin{Bmatrix} 1 \\ 2\cos n\psi \\ 2\sin n\psi \end{Bmatrix} d\psi \qquad (20)$$

and $B_0^k$, $B_{nc}^k$, and $B_{ns}^k$ are constant matrices of size $n$ by $n$; a total of $(2n_D + 1)$ such matrices arise from Eq. (19). A total of $n_T$ Fourier expansion are required to describe the sensitivity of the $B(\psi)$ matrix to changes in all of the $n_T$ trim variables. The calculation of these $(2n_D + 1)n_T$ matrices is straightforward, but the storage requirements may be substantial.

In an aeroelastic stability and response analysis, a substantial portion of the computational effort is spent in the calculation of the linearized, time-varying system matrix $B(\psi)$ at the required number of blade azimuth angles. Therefore, the calculation of each of the Fourier expansions represented by Eq. (19) can be considered essentially equivalent to one aeroelastic stability analysis from a computational cost standpoint. This means that to take into account the nonlinear terms in the sensitivity equation [Eq. (7)] one needs to carry out as many aeroelastic analyses as the number of elements $n_T$ of the trim vector. In many problems of realistic complexity $n_T$ can be larger than 20–30. These aeroelastic analyses represent an overhead that has to be paid regardless of the number of design variables considered in the problem. Therefore, if the number of design variables is less than or equal to $n_T$, and if one wants to take into account both the linear and the nonlinear contributions, it is more efficient to calculate the sensitivity of the FTM using finite difference approximations. The semianalytical approach, on the other hand, becomes more efficient if the number of design variables is greater than $n_T$, because the number of overhead aeroelastic analyses does not change with the number of design variables.

The calculation of the sensitivity of the FTM including both the linear and the nonlinear contributions can be carried out in a way similar to that used to calculate the linear contribution only [Eq. (17)]. The only difference is that the partial derivative matrices that appear on the diagonal are replaced by the total derivative matrices defined by Eq. (7), i.e.,

$$\begin{Bmatrix} \overset{*}{z} \\ \overset{*}{z}_1 \\ \overset{*}{z}_2 \\ \vdots \\ \overset{*}{z}_{N_{DV}} \end{Bmatrix} = \begin{bmatrix} D(\psi) & 0 & 0 & \cdots & 0 \\ D(\psi) & \dfrac{dD(\psi)}{dp_1} & 0 & \cdots & 0 \\ D(\psi) & 0 & \dfrac{dD(\psi)}{dp_2} & \cdots & 0 \\ \vdots & \vdots & \vdots & & \vdots \\ D(\psi) & 0 & 0 & \cdots & \dfrac{dD(\psi)}{dp_{N_{DV}}} \end{bmatrix} \begin{Bmatrix} z \\ z_1 \\ z_2 \\ \vdots \\ z_{N_{DV}} \end{Bmatrix} \qquad (21)$$

## Mathematical Model of the Helicopter

The method presented in the previous sections will be applied to the calculation of the sensitivity of the characteristic exponents of the mathematical model of a helicopter in forward flight. The model has been described extensively in the literature,[5,7,8] and only a brief summary of its main features will be presented here.

The mathematical model describes the coupled dynamics of main rotor, fuselage, and main rotor inflow. In particular, the inertia and aerodynamic blade loads because of rigid motions of the fuselage are taken into account. The rotor blades are modeled as isotropic, Bernoulli–Euler beams undergoing coupled flap-lag-torsional motion. Moderately large elastic deflections are assumed, therefore, the partial differential equations of motion of the blades are nonlinear due to nonlinear terms arising from the kinematics of deformation. The model includes steady stall, which could cause additional nonlinearities, but only linear incompressible aerodynamics is used in this study. A three-state model[9] is used to describe inflow dynamics. The partial differential equations of motion of the blades are transformed into a system of ODE using a finite element discretization based on Galerkin's method of weighted residuals.[10] A modal coordinate transformation based on the lowest frequency, coupled, rotating modes of an isolated rotor blade provides the means for both the assembly of the finite elements that make up the blade model, and a reduction of the number of rotor degrees of freedom. The modal coefficients take the place of the nodal coordinates as the generalized coordinates of the rotor portion of the model. The resulting equations, together with the system of ODE describing the six-degree-of-freedom rigid-body motion of the aircraft, and the ODE describing the dynamics of the main rotor inflow, make up the system of nonlinear, coupled rotor-fuselage-inflow equations of motion.

The solution process is composed of two parts. The first part consists of the determination of the trim state of the helicopter. The generic flight condition considered is a steady, coordinate, helical turn, defined by the magnitude of the velocity vector, the turn rate, and the flight-path angle. Straight and level flight is considered as a special case of turn with zero turn rate and flight-path angle. This includes the calculation of the steady-state equilibrium position of the main rotor blades. For this purpose, the equations of motion of one blade are transformed from ODE into a system of nonlinear algebraic equations using a classical Galerkin method.[7] A set of nonlinear algebraic equations for the fuselage enforces force and moment equilibrium in unaccelerated flight and other kinematic relations that are supposed to hold in a steady turn. The solution of the trim problem yields the steady-state inertia and aerodynamic attitudes of the helicopter, the pitch control settings, the steady average values of main rotor and tail rotor inflow, and the coefficients of the harmonics of the generalized coordinates of the blade.

The second step of the solution process consists of the determination of the aeromechanic stability of the coupled rotor–fuselage system and of the steady-state equilibrium position. The solution is based on a quasilinearization algorithm, which is an iterative, Newton-type method that converts the problem of solving a system of nonlinear ODE into that of solving a sequence of linear ODE.[5] These linear ODE arise from the linearization of the nonlinear system about the equilibrium position represented by the solution of the previous iteration. The sequence of linear solutions converges to the solution of the original nonlinear system. The FTM is also calculated at each iteration as part of the determination of the initial conditions for the linear system of ODE. In the present study, the steady-state equilibrium position is calculated in the trim step with sufficient numerical accuracy to be considered exact. This equilibrium position is used as an initial guess for the quasilinearization iteration, which therefore converges in exactly one step.

The equation of motion of the blades are formulated and linearized in a rotating coordinate system. In typical applications of the present model, the linearized equations would be converted to a nonrotating frame using a multiblade coordinate transformation.[8] Therefore, the rotor contributions to the state matrix $[B(\psi)]$ in Eq. (11) would be typically defined in a nonrotating system. The multiblade coordinate transformation tends to reduce considerably the periodicity of the state matrix, to the point that a constant coefficient approximation to $[B(\psi)]$ is usually sufficiently accurate for advance ratios $\mu$ below about 0.3. In the present study, the transformation is not carried out, so as to retain the strength of the parametric excitation.

## Results

The results presented in this section refer to a baseline four-bladed hingeless soft-in-plane rotor configuration with funda-

mental, rotating, coupled natural frequencies of 0.71/rev and 1.14/rev in lag and flap, respectively. The blades have uniform mass and stiffness properties along the span. The thrust coefficient of the helicopter is $C_T = 0.005$ and the rotor solidity is $\sigma = 0.07$. The blade has no precone, built-in twist or cross-sectional offset from the elastic axis. The rotor blade chord is $c = 0.055R$, the lift curve slope of the airfoil is $a = 6.28$, the profile drag coefficient of the airfoil is $c_{d0} = 0.01$, and the Lock number for the baseline case is $\gamma = 5.0$. The total number of states is 59, divided as follows: 12 states for each of the four blades (six coupled modes are used for the modal coordinate transformation of the blade degrees of freedom), eight fuselage states (the heading state is not included), and three dynamic inflow states. The typical computer time required for one coupled trim solution and for an aeromechanic stability and response analysis are about 3 and 15 min, respectively, on a Sun SPARCstation 2.

Two perturbations are considered in this study, namely a perturbation of 1% of the mass per unit span $m$, and a perturbation of slightly less than 1% of the blade torsional stiffness $GJ$. These values were selected based on the results of Ref. 6, which show that perturbations of this size are small enough to provide an accurate forward finite difference estimate of the gradients, but not so small that errors appear due to numerical cancellation and to insufficiently tight convergence of the underlying quasilinearization iteration. For each case, four flight conditions were considered, namely straight and level flight at advance ratios $\mu = 0.1$, 0.2, 0.3, and 0.4. In the discussion that follows, the finite difference approximations of the gradients will be considered as the exact values, with which the semianalytical values will be compared. Although the method described in this article generates simultaneously the sensitivities of both real and imaginary parts of the characteristic exponents, only results for the real parts will be presented here. In helicopter applications the real parts are by far the more important, because they are representative of the damping of the system. The imaginary parts are often ignored.

The first set of results refers to the linear contribution to the gradients that is on the partial derivative term in Eq. (7). The finite difference gradients used for comparison purposes are calculated by analyzing the perturbed design with the same trim and steady-state blade response as the baseline design. Figure 1 compares the sensitivities of the characteristic exponents to change in the distributed blade mass $m$ obtained using the semianalytical method of this study, with the corresponding finite difference values. The advance ratios are $\mu = 0.1$ and 0.4. The results are plotted in such a way that if the semianalytical and the finite difference predictions of the sensitivities are identical, the representative points on the figure will lie on the diagonal of the plot. This type of graphical representation was chosen because of the large number of predictions to be compared. For each value of the advance ratio there are 59 poles, several of which appear in closely spaced clusters. Two lines in the figure define a sector in which the relative error between the semianalytical and the finite difference predictions is less than ±5%. Figure 1 shows that most of the semianalytical predictions fall within the ±5% sector. Similar results were obtained for $\mu = 0.2$ and 0.3. The portions of the plots near the origin are expanded in Figs. 2 and 3, for advance ratios of $\mu = 0.1$ and 0.4, respectively. In these figures, sectors for ±5, ±10, and ±20% relative errors are marked. The enlarged plots show that although a few semianalytical predictions show slightly larger errors, most fall within the ±20% sector. A comparison of semianalytical and finite difference gradients for perturbations of torsion stiffness $GJ$ is presented in Fig. 4. The advance ratios are again $\mu = 0.1$ and 0.4. With the exception of a few characteristic exponents for the $\mu = 0.4$, the semianalytical sensitivities are within ±5% of the finite difference values. This is further confirmed by Fig. 5 in which the region near the origin is shown enlarged.

The calculation of the gradients would typically occur in the context of some sort of optimization procedure. Therefore it is important that the signs of the predicted gradients be the correct ones, so that the optimization algorithm can drive the design in the appropriate direction. This requirement is satisfied for all the components of the gradients, for perturbations of both $m$ and $GJ$. For helicopter applications, behavior constraints would typically be placed on the real parts of the characteristic exponents to ensure that the stability of the system

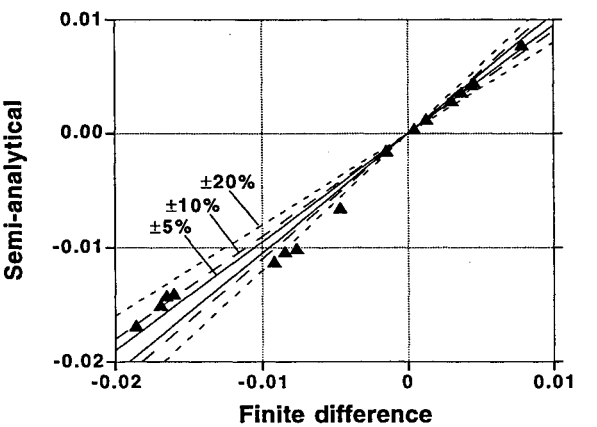


**Fig. 2 Comparison of semianalytical and finite difference derivatives of characteristic exponents with respect to $m$; linear contribution only. Advance ratio $\mu = 0.1$; enlarged view.**

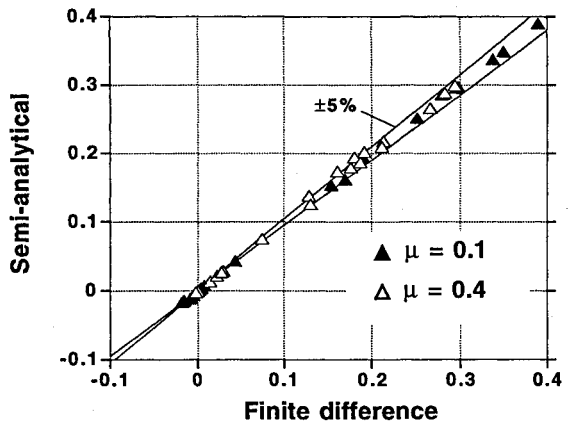


**Fig. 1 Comparison of semianalytical and finite difference derivatives of characteristic exponents with respect to $m$; linear contribution only.**

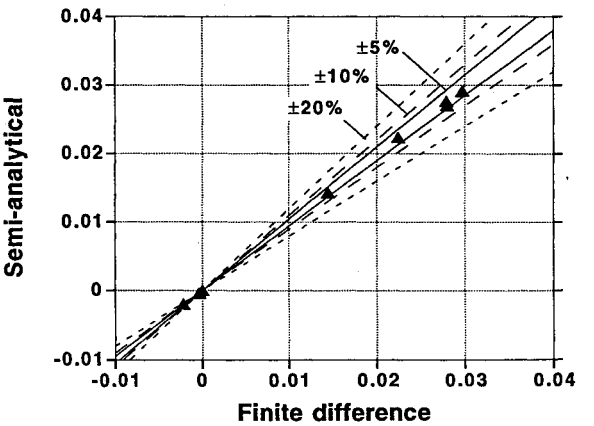


**Fig. 3 Comparison of semianalytical and finite difference derivatives of characteristic exponents with respect to $m$; linear contribution only. Advance ratio $\mu = 0.4$; enlarged view.**

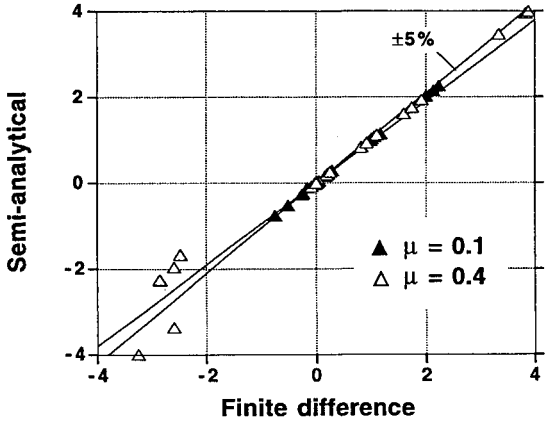


Fig. 4 Comparison of semianalytical and finite difference derivatives of characteristic exponents with respect to *GJ*; linear contribution only.

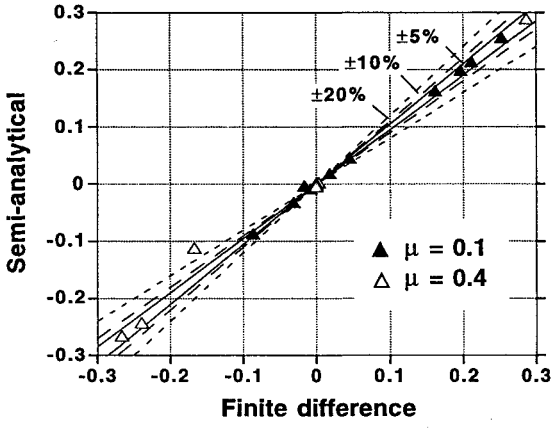


Fig. 5 Comparison of semianalytical and finite difference derivatives of characteristic exponents with respect to *GJ*; linear contribution only; enlarged view.

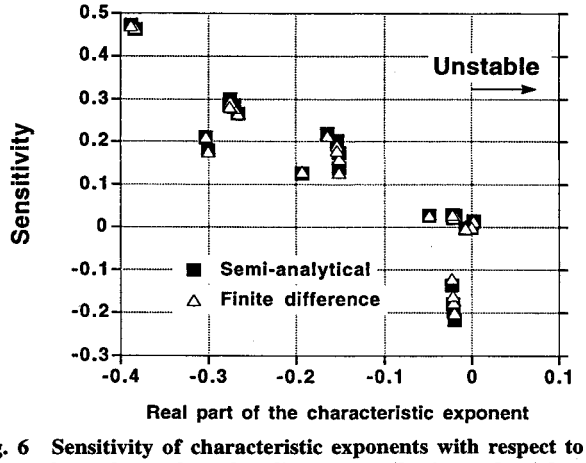


Fig. 6 Sensitivity of characteristic exponents with respect to *m* for the least damped modes; linear contribution only. Advance ratio $\mu = 0.4$.

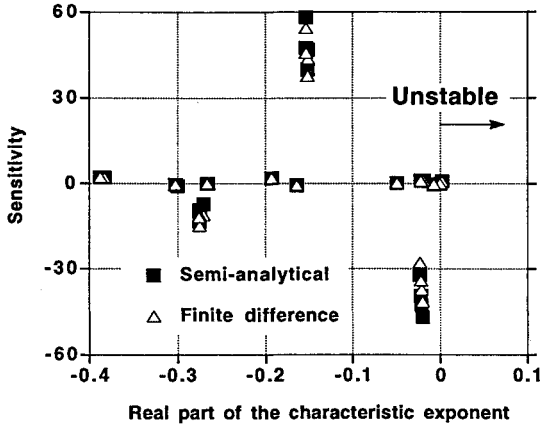


Fig. 7 Sensitivity of characteristic exponents with respect to *GJ* for the least damped modes; linear contribution only. Advance ratio $\mu = 0.4$.

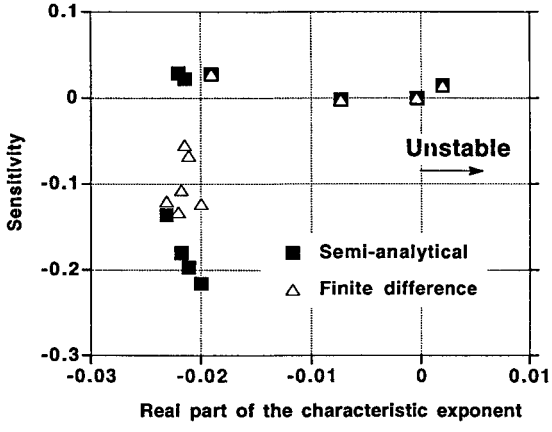


Fig. 8 Sensitivity of characteristic exponents with respect to *m* for the least damped modes; linear contribution only. Finite difference data results obtained using raw characteristic exponents. Advance ratio $\mu = 0.4$.

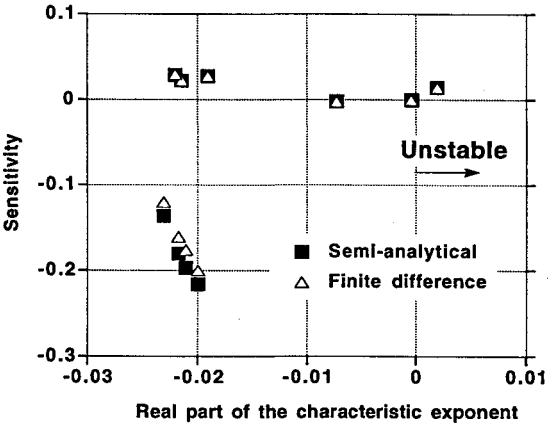


Fig. 9 Sensitivity of characteristic exponents with respect to *m* for the least damped modes; linear contribution only. Finite difference data results obtained using sorted characteristic exponents. Advance ratio $\mu = 0.4$.

be preserved during the optimization. Figures 6 and 7 show the sensitivity as a function of the real part of the characteristic exponents for perturbations of *m* and *GJ*, respectively, at an advance ratio $\mu = 0.4$. There is a very good match between the analytical and the finite difference sensitivities for most of the characteristic exponents shown in the figures.

Figure 8–11 compare finite difference and semianalytical sensitivities for the 10 lowest damping modes. The accuracy of the predictions for these modes would obviously be especially important in an optimization process. These figures illustrate a potential pitfall of the use of finite difference based gradients. In the computer implementation of this study, the characteristic exponents are output sorted by real parts. The finite difference sensitivities are then built using the real parts of the characteristic exponents in the same position of the output for the perturbed configuration and for the baseline con-

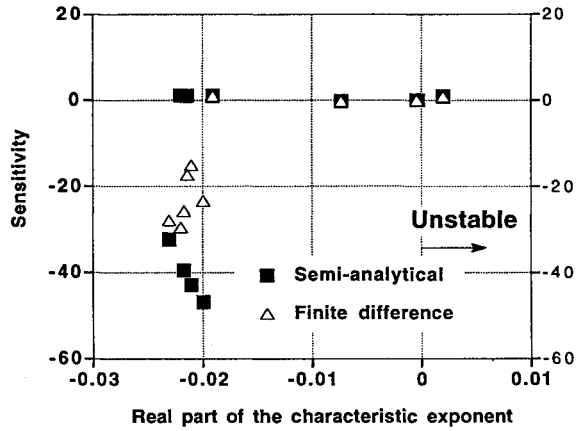


**Fig. 10 Sensitivity of characteristic exponents with respect to *GJ* for the least damped modes; linear contribution only. Finite difference data results obtained using raw characteristic exponents. Advance ratio $\mu = 0.4$.**

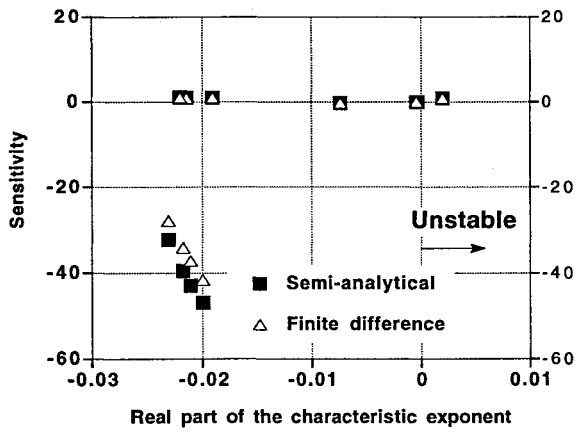


**Fig. 11 Sensitivity of characteristic exponents with respect to *GJ* for the least damped modes; linear contribution only. Finite difference data results obtained using sorted characteristic exponents. Advance ratio $\mu = 0.4$.**

figuration. The results of this process are shown in Fig. 8 for a perturbation of the distributed mass $m$. The agreement is excellent for four of the 10 characteristic exponents shown in the figure, but only fair for the remaining six. When sorted by real parts, these six exponents are clustered close together. More troublesome, the finite difference and the semianalytical predictions have the opposite sign for two of the exponents. This means that if these gradients were used in an optimization procedure the optimizer might be driven into the wrong direction. The reason for this problem is that, when sorted by real parts, some exponents switch positions between the baseline and the perturbed configurations. In other words, using the $k$th item of the baseline and of the perturbed output list of exponents does not guarantee that one is using the baseline and the perturbed value of the $k$th characteristic exponent. Thus, to carry out a correct comparison between semianalytical and finite difference gradients the following approach was used instead. Using the baseline value $\lambda_k$ and the semianalytical gradient $\partial\lambda_k/\partial p$, a predicted value $\lambda_{kP}$ was calculated for the perturbed value of $\lambda_k$ as

$$\lambda_{kP} = \lambda_k + \frac{\partial \lambda_k}{\partial p}\Delta p$$

Then the characteristic exponent of the perturbed configuration closest to $\lambda_k$ was selected as the exponent to be used for the finite difference calculation. The results of this sorting procedure are shown in Fig. 9. The agreement is now excellent for six of the 10 exponents, corresponding to aircraft rigid body and inflow modes, and very good for the remaining four, corresponding to the first lag mode for each of the four blades. More importantly, all of the gradients have the correct sign. Exactly the same behavior can be observed when *GJ* is perturbed, as shown in Figs. 10 and 11 for the raw and sorted finite differences, respectively. Obviously the procedure just outlined could not be used in practice to calculate correct finite difference gradients because semianalytical gradients would clearly not be available. For the cases of this study, none of the following sorting criteria generated a consistent list of characteristic exponents between the baseline and the perturbed configurations: 1) real part or 2) imaginary part of the characteristic exponent, 3) real part or 4) imaginary part, or 5) absolute value of the corresponding characteristic multiplier. The semianalytical method does not have this problem because it intrinsically contains eigenvector information, and therefore the correct gradient is always obtained. The derivation of a reliable sorting algorithm to be used in finite difference gradient calculations was outside the objectives of this study and was not attempted. It is quite likely, however, that such an algorithm will require the use of the eigenvectors of the FTM. It is possible that the only reliable way of calculating finite difference gradients of the characteristic exponents is to calculate the finite difference gradients of the FTM and then calculate the gradients of the characteristic exponents analytically, using Eqs. (4–6).

Because of the substantial cost of calculating the full value of the sensitivities, that is, including the effect of trim changes, it is important to determine whether the linear contributions alone can provide sufficiently accurate estimates of the full gradient. Figures 12 and 13 compare the linear and the nonlinear gradients with respect to $m$ and *GJ*, respectively. Both types of gradients are calculated using finite difference approximations. Each figure shows results for advance ratios $\mu = 0.1$ and 0.4. The value $\mu = 0.4$ is representative of the highest levels of parametric excitation and of nonlinearity that the mathematical model is going to predict. Therefore, in light of the fact that most of the linear sensitivities appear to be within ±5% of the full nonlinear values, it can be concluded that it is acceptable to neglect the effects of changes in the equilibrium position about which the equations of motion are linearized. The sensitivities of the 10 least-damped modes are shown in Figs. 14 and 15 for perturbations of $m$ and *GJ*, respectively, and for $\mu = 0.4$. Both figures confirm that linear gradients are likely to be sufficiently accurate. Especially important is the fact that the linear approximation appears to maintain the correct sign of all the gradients. On the other hand, the intrinsic limitations of the mathematical model should be kept in mind. For example, in the results of this

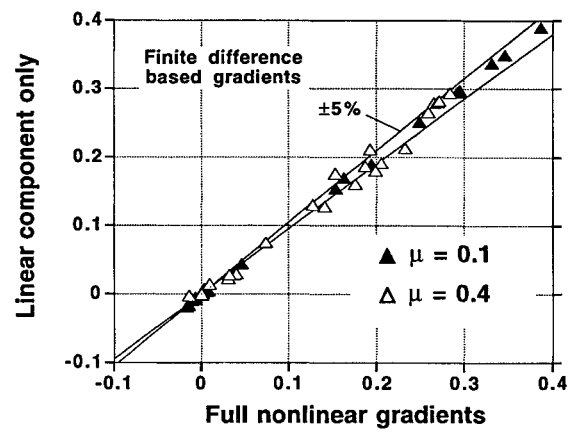


**Fig. 12 Comparison of linear (not retrimmed) and nonlinear (retrimmed) sensitivities of characteristic exponents with respect to *m*.**

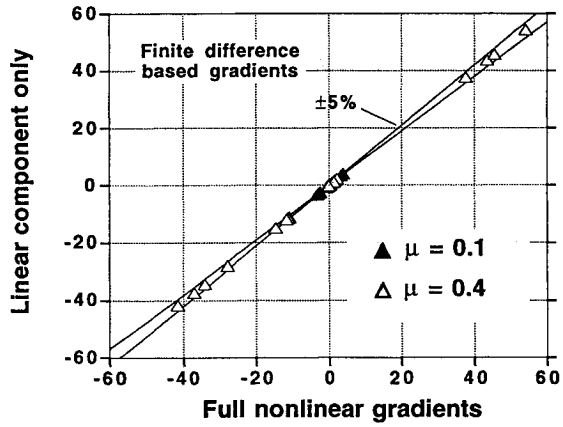


**Fig. 13 Comparison of linear (not retrimmed) and nonlinear (retrimmed) sensitivities of characteristic exponents with respect to *GJ*.**

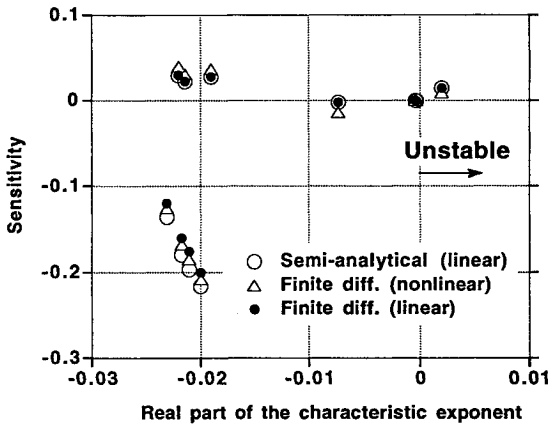


**Fig. 14 Sensitivity of characteristic exponents with respect to *m* for the least damped modes. Advance ratio $\mu = 0.4$.**

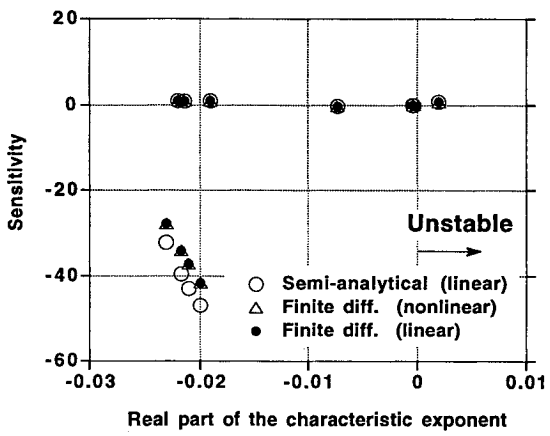


**Fig. 15 Sensitivity of characteristic exponents with respect to *GJ* for the least damped modes. Advance ratio $\mu = 0.4$.**

study all the nonlinearities are due to the geometry of deformation of the blades. These nonlinearities tend to be relatively weak. The model does not include any nonlinearities of aerodynamic origin, such as stall and compressibility, that can be significant in certain flight conditions. Even geometric nonlinearities could be substantially stronger if, for example, the blade was much softer in torsion. Therefore, although the mathematical model used for the aeroelastic analysis is sufficiently accurate to be realistic, its intrinsic limitations should be kept in mind when generalizing the conclusions of this study.

## Conclusions

This article has presented a methodology for the calculation of the gradients of the characteristic exponents of a linearized system with periodic coefficients, using semianalytical derivatives rather than finite difference approximations. Two contributions to the gradients are identified. The first is associated with changes in the time-varying system matrix because of changes in the design parameters, while keeping unchanged the steady-state equilibrium position about which the equations are linearized; this can be considered as a linear contribution. The second is associated with the changes in the steady-state equilibrium position, and can be considered as a nonlinear contribution.

The results obtained in this study indicate the following:

1) Semianalytical sensitivities of the characteristic exponents with respect to one design parameter can be obtained for a fraction of the cost of one stability analysis, if one neglects the effects of changes in equilibrium position. Attention should be paid to the details of the implementation, so that the cost of solving the system of ODE that provide the sensitivities does not grow to the point of negating the computational advantages of the semianalytical formulation.

2) The cost of taking into account the effects on the characteristic exponents of changes in the equilibrium position about which the nonlinear ODE are linearized is substantial. The additional cost is equal to the cost of as many analyses as the number of parameters that define the trim condition. This cost, however, is essentially independent of the number of design variables. Therefore, semianalytical sensitivity analyses that include the effects of trim changes can become competitive with finite difference based calculations only for larger problems. For analyses such as that of this article, the break-even point is of about 40–50 design variables.

3) The examples presented in this article indicate that it is possible to neglect the effect of trim changes without any great loss of accuracy. This is probably a general conclusion, as long as the strength of the nonlinearities remains comparable to that of the examples. If the system becomes substantially more nonlinear, for example, because the torsional stiffness of the blade is very low, or because extensive nonlinear aerodynamic phenomena are present, this conclusion may have to be re-evaluated.

4) If the gradients are calculated using finite difference approximations, great care must be taken in using the baseline and the perturbed characteristic exponents corresponding to the same mode, especially if the characteristic exponents appear in poorly separated clusters. It may be impossible to perform a correct identification automatically, or even manually, based only on the characteristic exponents themselves, and eigenvector information may have to be used. An erroneous identification may lead to gradients that have the wrong sign, and therefore might drive an optimization procedure in the wrong direction. It is advisable to calculate the gradient of the FTM using finite differences and then obtain the sensitivities of the characteristic exponents analytically. The semianalytical sensitivity approach described in the article does not experience any such problems.

## Acknowledgments

This work was supported by the Army Research Office, Contract DAAL-03-88-C-002, Technical Monitor Tom Doligalski. Partial support was also provided by the NSF Engineering Research Centers Program NSFD-CDR-88-03012.

## References

[1]Lim, J. W., and Chopra, I., "Stability Sensitivity Analysis of a Helicopter Rotor," *AIAA Journal*, Vol. 28, No. 6, 1990, pp. 1089–1097.

[2]Lu, Y., and Murthy, V. R., "Sensitivity Analysis of Discrete Periodic Systems with Applications to Helicopter Rotor Dynamics,"

*AIAA Journal*, Vol. 30, No. 8, 1992, pp. 1962–1969.

[3]Johnson, W., *Helicopter Theory*, Princeton Univ. Press, Princeton, NJ, 1980, pp. 369–377.

[4]Haftka, R. T., Gurdal, Z., and Kamat, M. P., *Elements of Structural Optimization, 2nd Ed.*, Kluwer Academic, Norwell, MA, 1990, pp. 235–238.

[5]Celi, R., and Friedmann, P. P., "Rotor Blade Aeroelasticity in Forward Flight with an Implicit Aerodynamic Formulation," *AIAA Journal*, Vol. 26, No. 12, 1988, pp. 1425–1433.

[6]Spence, A., and Celi, R., "Efficient Sensitivity Analysis for Rotary-Wing Aeromechanical Problems," *Proceedings of the AIAA/ASME/ASCE/AHS 34th Structures, Structural Dynamics, and Materials Conference* (La Jolla, CA), AIAA, Washington, DC, 1993, pp. 3012–3022.

[7]Celi, R., "Hingeless Rotor Dynamics in Coordinated Turns," *Journal of the American Helicopter Society*, Vol. 36, No. 4, 1991, pp. 39–47.

[8]Spence, A., and Celi, R., "Coupled Rotor-Fuselage Dynamics in Turning Flight," *Proceedings of the AIAA Dynamics Specialist Conference* (Dallas, TX), AIAA, Washington, DC, 1992, pp. 292–301.

[9]Peters, D. A., and HaQuang, N., "Dynamic Inflow for Practical Applications," *Journal of the American Helicopter Society*, Vol. 33, No. 4, 1988, pp. 64–68.

[10]Friedmann, P. P., and Straub, F. K., "Application of the Finite Element Method to Rotary-Wing Aeroelasticity," *Journal of the American Helicopter Society*, Vol. 25, No. 1, 1980, pp. 36–44.